

1995/21557

COMPARATIVE PERFORMANCE TESTS ON THE MOD-2,
2.5-MW WIND TURBINE WITH AND WITHOUT VORTEX GENERATORS*

G. E. Miller

N95-27978

Boeing Aerospace Company
Seattle, Washington 98124

ABSTRACT

A test program was conducted on the third Mod-2 unit at Goldendale, Washington, to systematically study the effect of vortex generators (VG's) on power performance. The subject unit was first tested without VG's to obtain baseline data. Vortex generators were then installed on the mid-blade assemblies, and the resulting 70% VG configuration was tested. Finally, vortex generators were mounted on the tip assemblies, and data was recorded for the 100% VG configuration. This test program and its results are discussed in this paper. The development of vortex generators is also presented.

NOMENCLATURE

AEP	Annual Energy Production
BPA	Bonneville Power Administration
Met	Meteorological
NACA	National Advisory Committee for Aeronautics
PGandE	Pacific Gas and Electric Company
PNL	Pacific Northwest Laboratories (Battelle)
Sta	Radial Station (Inches)
VG	Vortex Generator
WTS	Wind Turbine System

INTRODUCTION

Analytical studies using wind tunnel data as input indicated that vortex generators could be used to increase Mod-2 power performance in below-rated operation. Subsequent tests conducted on the PGandE Mod-2 unit located in Solano County, California, demonstrated that power performance was improved substantially by installing VG's on the mid-blade assemblies. The Solano test results will be published by PGandE through the Electric Power Research Institute.

Later, in support of the Mod-5B program, it became necessary to confirm that a larger improvement in power performance could be obtained if VG's were mounted on both the mid-blade and tip assemblies. Therefore, a test program was planned and conducted to systematically study the effect of VG spanwise extent on Mod-2 power performance. This test program and its results are presented in this paper. First, however, the development of vortex generators will be discussed.

VORTEX GENERATOR DEVELOPMENT

A variety of vortex generating devices have been developed for boundary layer control over the past 35 years or so. In Reference 1, Pearcy describes several types of vortex generators and discusses their application to the prevention of shock-induced boundary layer separation. When this phenomenon

*Presented at the DOE/NASA Workshop on Horizontal Axis Wind Turbine Technology, May 8-10, 1984 in Cleveland, Ohio.

occurs on the wings of high speed aircraft, additional drag is produced and the aircraft's stability and control may be adversely affected. Vortex generators are often mounted on the wings of jet transports to delay flow separation and prevent the occurrence of control problems.

The majority of wind turbine rotors do not encounter shock-induced boundary layer separation because they operate in the incompressible flow regime. The Mod-2 rotors, however, experience another type of boundary layer separation that begins at the trailing edge and progressively moves forward along the suction surface as the angle of attack increases. This type of separation occurs when the boundary layer can no longer follow the blade surface as it traverses a region on which an adverse pressure gradient is imposed by the external flow. With increasing angle of attack below stall, this separation process results in gradual loss of lift and an additional, undesirable drag increment. This separation process also results in the gentle trailing edge stall that is characteristic of most thick airfoils.

The fixed pitch Mod-2 mid-blade assemblies utilize thick airfoils that are required to function at large angles of attack throughout much of the operational wind speed range. Therefore, the power production of the mid-blade assemblies is limited primarily by this separation process. The power production capability of the mid-blade assemblies could be improved if the stall angle and maximum lift of these airfoils could be increased by delaying the boundary layer separation process.

To achieve this goal, Boeing conducted a series of wind tunnel tests to explore the use of vane-type vortex generators as high lift devices on thick airfoils operating in flow conditions appropriate to large horizontal axis wind turbines. Initially, corotational and counterrotational VG patterns were studied. These two patterns are illustrated in Figure 1. For the same vane size and spacing, counterrotational VG's were slightly more effective in generating maximum lift than corotational VG's. Therefore, most of the testing was directed toward optimizing the counterrotational configuration.

The VG pattern found to be most effective in producing maximum lift is illustrated in Figure 2. This high lift VG pattern uses the larger of the two vane sizes shown and was used to design the mid-blade VG's. The effect of this high lift VG pattern on the lift and drag characteristics of a 24 % thick airfoil is presented in Figure 3. Note that the vortex generators increased the lift over the entire angle of attack range shown. Also note that the stall angle is increased by 6 degrees and the maximum lift is increased by 90%. The minimum drag penalty for this VG installation is only 20 counts. For lift coefficients greater than 0.7, however, the drag is lower with the VG's installed.

The second, smaller vane shown in Figure 2 was also developed in the wind tunnel. Relative to the results obtained with the larger VG's, the smaller VG's produced 5% less maximum lift; but the minimum drag penalty is reduced by 70%. The smaller VG's were developed for application to the blade tips which always operate below stall. Consequently, maximum lift is of secondary importance; however, any additional drag resulting from premature boundary layer separation is undesirable. Premature boundary layer separation could be triggered by distributed roughness or manufacturing contour imperfections, especially when located near the leading edge. For a given operating pitch schedule, the smaller VG's would produce a net drag reduction and some additional lift so that the power contribution from the tip assemblies is increased.

Before proceeding into the discussion of the Mod-2 test, a brief discussion of vortex generator physics will be presented. In the literature, the interaction of the VG's with the boundary layer on the mounting surface is described as a mixing process between the high energy external flow and the low energy boundary layer fluid. This mixing process reenergizes the boundary layer allowing it to follow the airfoil surface for a greater distance into a region with an adverse pressure gradient before separation occurs.

Flow visualization studies were included in the Boeing wind tunnel tests to examine this interaction process. The observed flow field for a well designed counterrotational VG pattern is illustrated in Figure 4. The observed flow field is very similar to that presented in Reference 1. As indicated in Figure 4, each vane produces a discrete vortex just outside the local boundary layer. As these vortices trail downstream, the vortices from toed-out vane pairs (looking toward the leading edge) gradually approach one another. The resulting vortex pairs generate a secondary flow which evacuates low energy fluid from the adjacent portions of the boundary layer. This low energy fluid is entrained by the viscous vortex cores. Simultaneously, the vortex pairs impress the high energy external flow against the adjacent portions of the boundary layer. Some high energy fluid is also entrained by the vortex cores. The effect of this secondary flow is to confine separation effects to the aft portion of the suction surface beneath the vortex pairs. As a result, lift capability is increased and form, or pressure, drag is reduced. At the higher angles of attack, wake surveys show a dramatic reduction in low energy wake fluid corresponding to a net drag reduction.

TEST DESCRIPTION

The subject test was conducted on the third Mod-2 unit, which is located on a site approximately 17 miles east of Goldendale, Washington. The first and second Mod-2 units are also located at this site. A general arrangement of the Goldendale site is illustrated in Figure 5. The test unit is situated near the southwest corner of the site. The two meteorological towers at the Goldendale site are also indicated in this figure.

A brief description of the test unit is presented in Figure 6. A detailed description of the Mod-2 WTS

is contained in Reference 2. Except for the vortex generator installations described below, the configuration of Unit #3 was not altered during the test.

The subject test was conducted during July and August, 1983. This test was conducted in parallel with another test which studied the effect of vortex generators on loads. The results of that test are presented in Reference 3.

At the beginning of the test, Unit 3 did not have vortex generators. This initial configuration was operated from July 8 through July 13, 1983, to obtain baseline data. Vortex generators were then installed on the mid-blade assemblies as illustrated in Figure 7. The resulting 70% VG configuration was operated from July 19 through July 28, 1983. Vortex generators were then installed on the tip assemblies as illustrated in Figure 8. The resulting 100% VG configuration was then operated from August 1 to September 1, 1983. However, most of the operational hours for the third configuration occurred during the first eight days of August.

DATA PROCESSING

During the test period, data from Unit #3 and the meteorological towers was recorded on magnetic tape for posttest processing. The various stages of the data processing sequence are discussed in this section.

The data tapes were first used to generate analog traces showing the beginning and end of each data run. These traces were used to determine start and stop times for power production. These traces also included the air pressure and temperature recorded from the BPA met tower. An average air density ratio for each data run was determined from these atmospheric parameters. The air density ratio was used to refer the measured generator power to standard sea level ambient conditions.

The power production interval of each run was then divided into convenient 10 minute intervals for digital processing. Smooth wind conditions were not considered in selecting the time intervals. At the beginning and end of each run, one minute intervals were also identified to provide a zero power check.

The appropriate data channels were then digitized during the 1 minute and 10 minute intervals. The digitizing rate was 10 samples per second. Next the mean value of each channel was calculated for each time interval. A zero power correction derived from the 1 minute intervals was then applied to the 10 minute average power levels. Finally, the 10 minute power levels were referred to standard sea level conditions using the following formula:

$$\text{Referred Power} = \text{Measured Power} / \text{Air Density Ratio}$$

During the test period, the air density ratio at the site was approximately 0.90. Therefore, the referred power is approximately 11% greater than the measured power. For measured power levels greater than approximately 2250 kW, this procedure will generate referred power levels greater than rated power. If the test unit were operating at a site with standard sea level ambient conditions, however, the control system would have trimmed the power

output for these data points to the rated level. Therefore, since the purpose of the power referral step is to derive the power-velocity curve for a sea level standard site, the referred power cannot be greater than rated power.

TEST RESULTS

The measured variations of power output with wind speed for the three configurations are first discussed separately. Then a comparison between the three power-velocity curves is presented. Standard sea level ambient conditions are assumed in this discussion. The power output was measured in the nacelle at the generator terminals. The wind speed was measured at the 195 ft. level on the BPA met tower.

A total of 72 power-velocity data points were obtained for the baseline configuration without VG's. These data points are presented in Figure 9. Most of these data points occur in the wind speed interval from 20 to 34 mph. Only a few data points were obtained at wind speeds less than 20 mph. The highest wind speed at which data was obtained is 34.8 mph. The distribution of data points with wind speed is shown in Figure 10.

Because of the noticeable data scatter, a least-squares polynomial curve fit was used to obtain the power variation with wind speed. A third order polynomial was selected as the best fit based upon minimization of the standard error. This curve fit and its formula are also shown in Figure 9.

The rated wind speed for the zero VG configuration is approximately 32 mph for standard sea level conditions. Note that the average generator power measured during rated power operation is only 2460 kW. The observed deviation of the measured rated power level from the 2500 kW power setpoint can be attributed to data system calibration error and pitch control dynamics.

A total of 78 power-velocity data points were obtained for the 70% VG configuration. These data points are plotted in Figure 11. Most of the data points occur within two wind speed intervals. The first interval is from 16 to 23 mph, and the second interval is from 29 to 36 mph. The data point distribution with wind speed is shown in Figure 12. The highest wind speed at which data was obtained is 37.3 mph.

The below-rated power data for the 70% VG configuration was approximated by applying a least-squares linear curve fit. A higher order curve fit could not be justified because of the small number of data points for wind speeds from 23 to 29 mph. The resulting curve fit and its formula are shown in Figure 11. From this curve fit, a rated wind speed of approximately 28.5 mph can be inferred for standard sea level conditions.

Several hours of rated power operation were recorded while testing the 70% VG configuration. The data points obtained from this data clearly show that the mean power output during rated power operation is 2460 kW.

A total of 49 power-velocity data points were obtained for the 100% VG configuration. These data points are presented in Figure 13. All of these data points occur in the wind speed interval from 16 to 30 mph. The data point distribution in Figure 14 shows that these data points are distributed fairly uniformly across this wind speed interval.

The below-rated power data for the 100% VG configuration was approximated by applying a least-squares polynomial curve fit. A linear curve fit was selected based upon minimization of the standard error. This curve fit and its formula are also shown in Figure 13.

The rated wind speed for the 100% VG configuration is approximately 27 mph. As noted for the other two configurations, the average power level for rated power operation is 2460 kW.

The curve fits to the power-velocity data for the three configurations are compared in Figure 15. When operating below-rated power, the 100% VG configuration produces the most power, while the no VG configuration produces the least power. The power output of the 70% VG configuration is approximately halfway between that of the other two configurations. The installation of the 70% VG's reduced the rated wind speed from approximately 32 mph to 28.5 mph. With the addition of the tip VG's, the rated wind speed was reduced further to approximately 27 mph. The minimum operating wind speed of approximately 13.8 mph is not affected by the VG installation.

The annual energy production (AEP) was also calculated for the three measured power-velocity curves. These AEP results are shown on Figure 15 relative to the baseline configuration without VG's. Note that the 100% VG configuration increased the AEP by 15.2%, while the 70% VG configuration resulted in an 8.6% AEP increase. The Mod-5B Weibull wind speed distribution shown in Figure 16 was used in these calculations.

Analytical studies using wind tunnel data as input support the AEP increment obtained for the 100% VG configuration. However, these studies indicate that the AEP increment for the 70% VG configuration should be approximately 2% greater. The discrepancy is believed to result from the lack of data for the 70% VG configuration for wind speeds from 23 to 29 mph. The few data points obtained in this wind speed interval agree quite well with predictions. Furthermore, excellent agreement between analysis and data was obtained for the 70% VG configuration tested at Solano.

SUMMARY

The results of this test program can be summarized as follows:

- 1) The Mod-2 power production in below-rated operation is maximized by installing vortex generators on both the mid-blade and tip assemblies.

- 2) For the Mod-5B Weibull wind speed distribution, the 100% VG configuration increased the annual energy production by 15.2%, while the 70% VG configuration resulted in an 8.6% AEP increase. Because of insufficient data, the AEP increment for the 70% VG configuration may be too low. Analytical studies indicate that the AEP increase for the 70% VG configuration is approximately 10.5%. This analytical prediction is consistent with the Solano data.

The results of this test program confirmed the design decision to install vortex generators on both the mid-blade and tip assemblies of the Mod-5B rotor.

REFERENCES

1. Pearcy, H. H., "Shock-Induced Separation and Its Prevention by Design and Boundary Layer Control," *Boundary Layer and Flow Control*, Vol. 2, ed. by Lachmann, G. V., Pergamon Press, New York, 1961.
2. Boeing Engineering and Construction Company, *Mod-2 Wind Turbine System Development Final Report, Volume 2 - Detailed Report*, NASA CR-168007, September 1982.
3. Zimmerman, D. K., Shipley, S. A. and Miller, R. D., "Comparison of Measured and Calculated Dynamic Loads for the Mod-2, 2.5-MW Wind Turbine System," presented at DOE/NASA Workshop on Horizontal Axis Wind Turbine Technology, May 8-10, 1984 in Cleveland, Ohio.

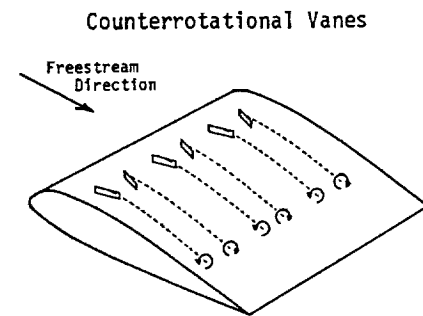
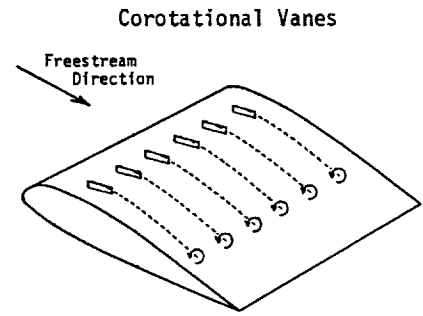


Figure 1. Comparison Of Corotational And Counterrotational Vane-type Vortex Generators.

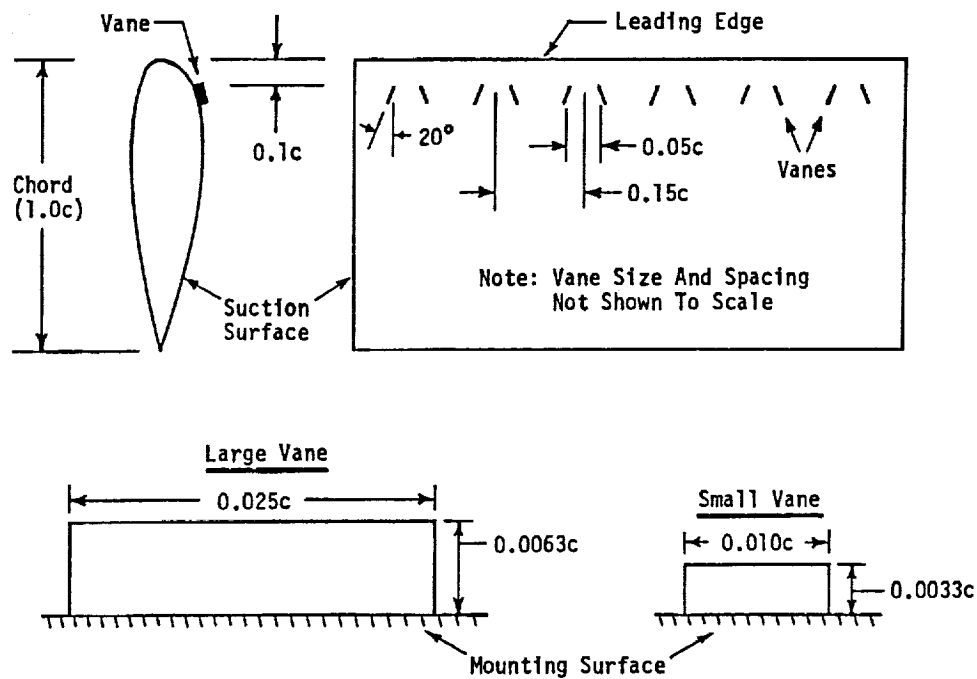


Figure 2. Counterrotational Vortex Generator Configurations.

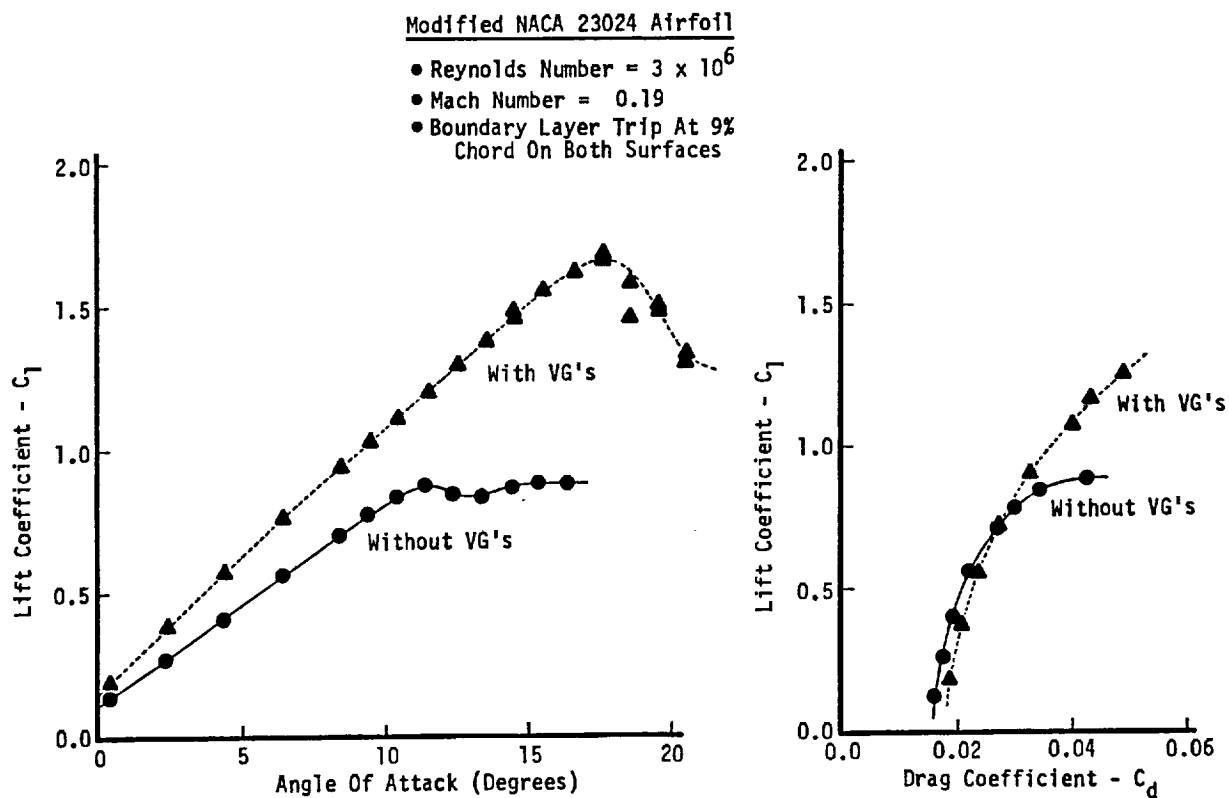


Figure 3. Effect Of Vortex Generators On Two-Dimensional Airfoil Lift And Drag Characteristics.

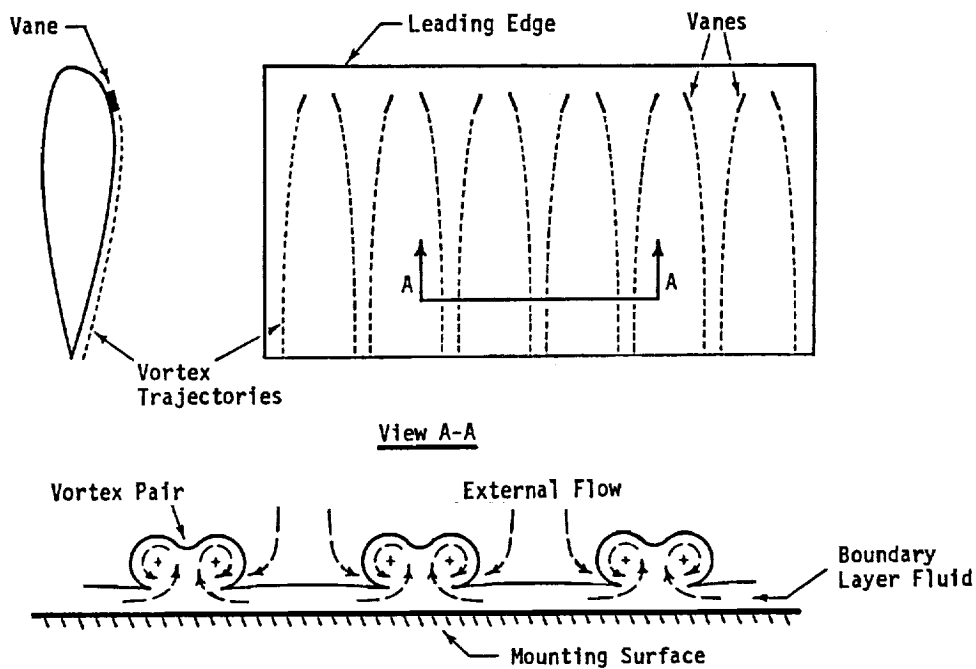


Figure 4. Observed Flow Structure For Counterrotational Vortex Generators.

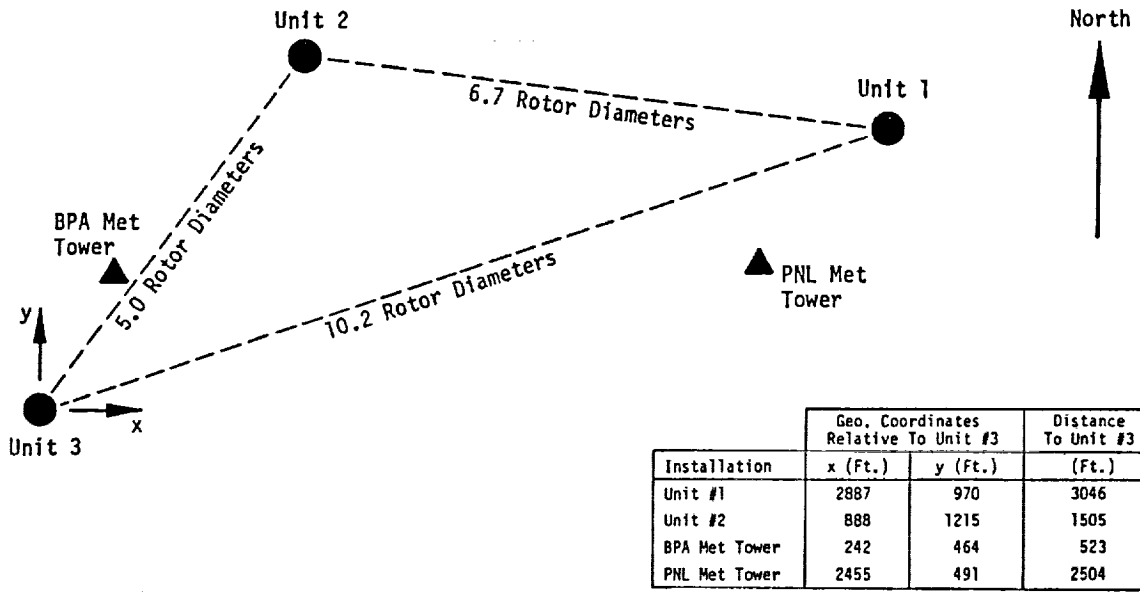


Figure 5. General Arrangement Of Goldendale Site.

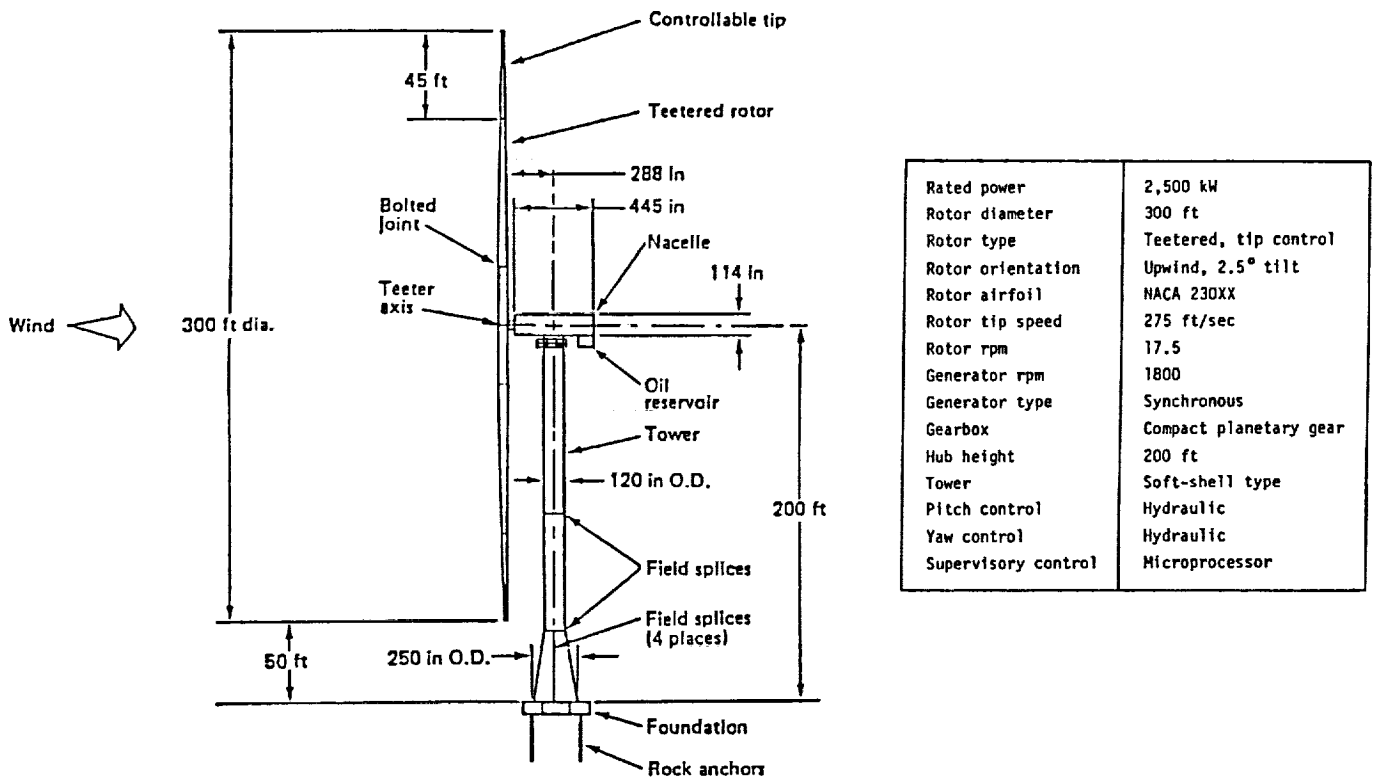


Figure 6. Description Of Mod-2 WTS.

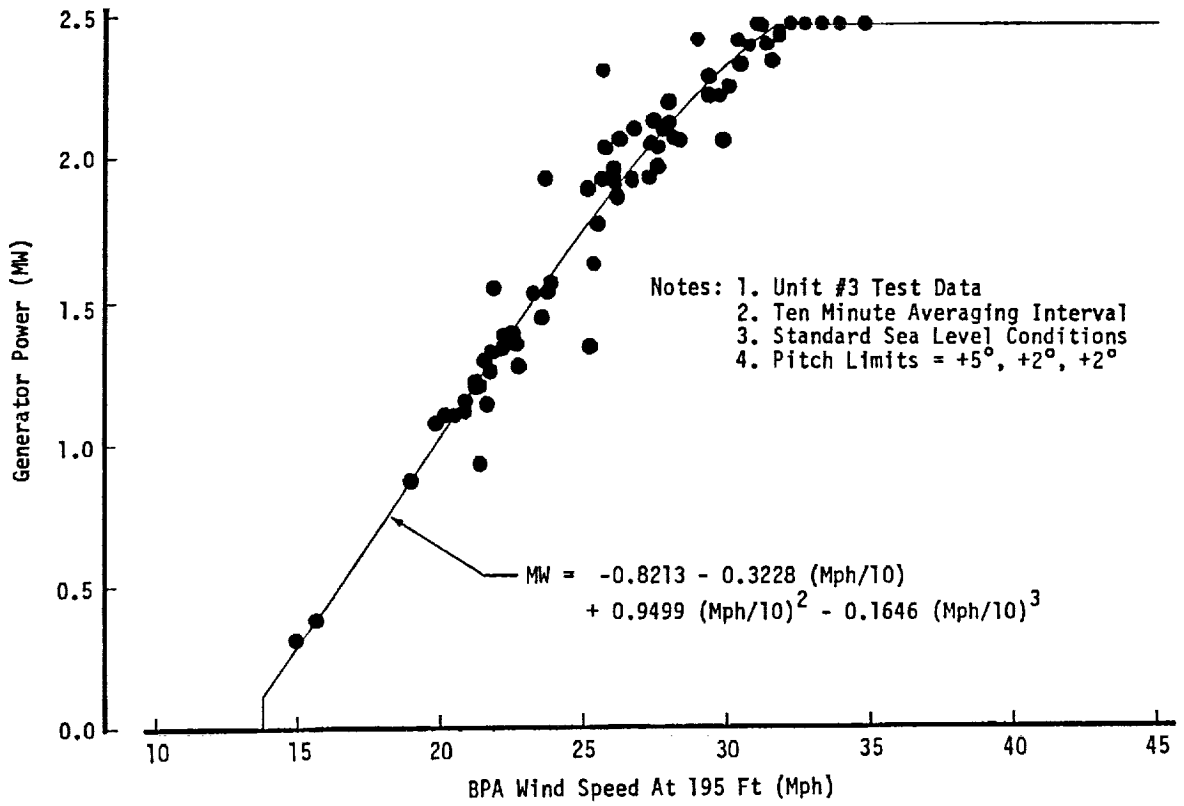


Figure 9. Mod-2 Power Performance Without Vortex Generators.

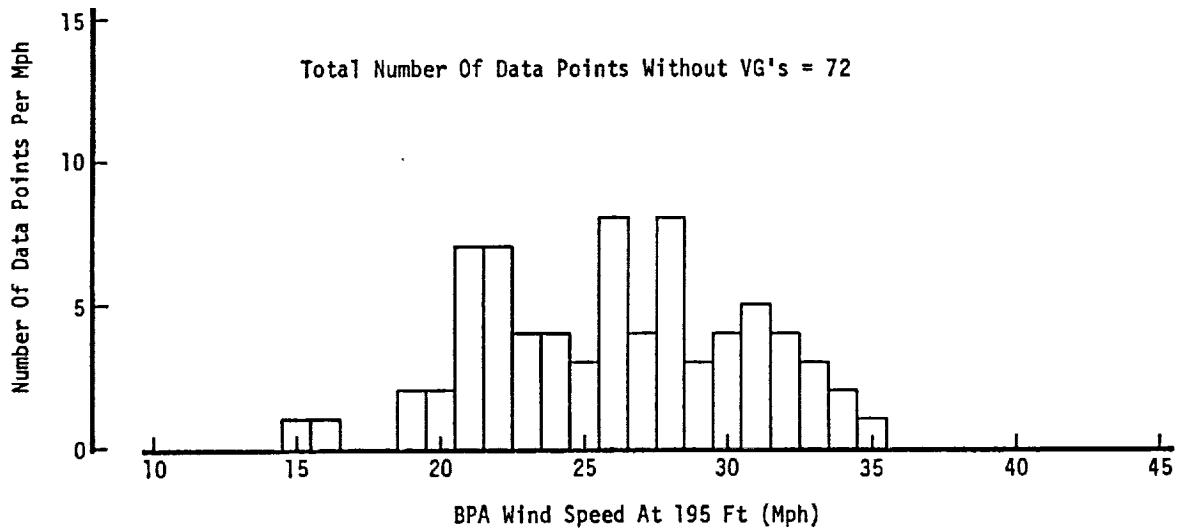


Figure 10. Data Point Distribution Without Vortex Generators.

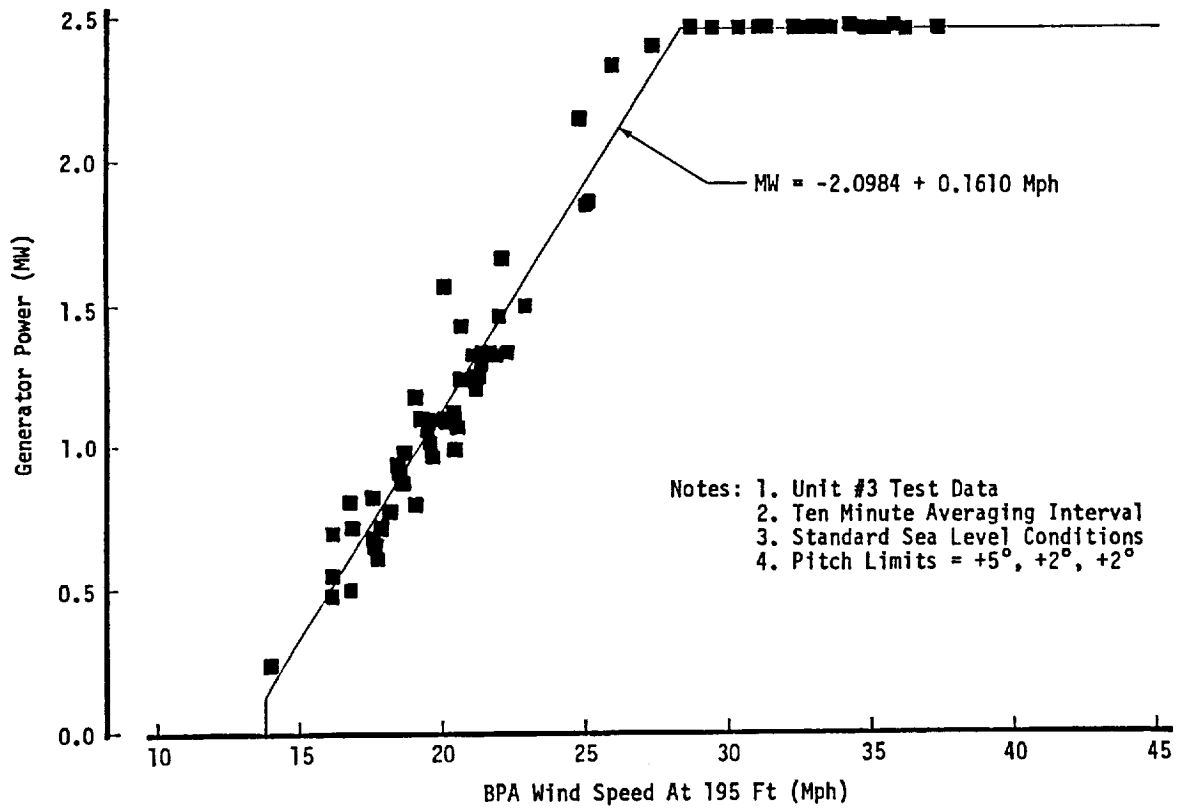


Figure 11. Mod-2 Power Performance With 70% Vortex Generators.

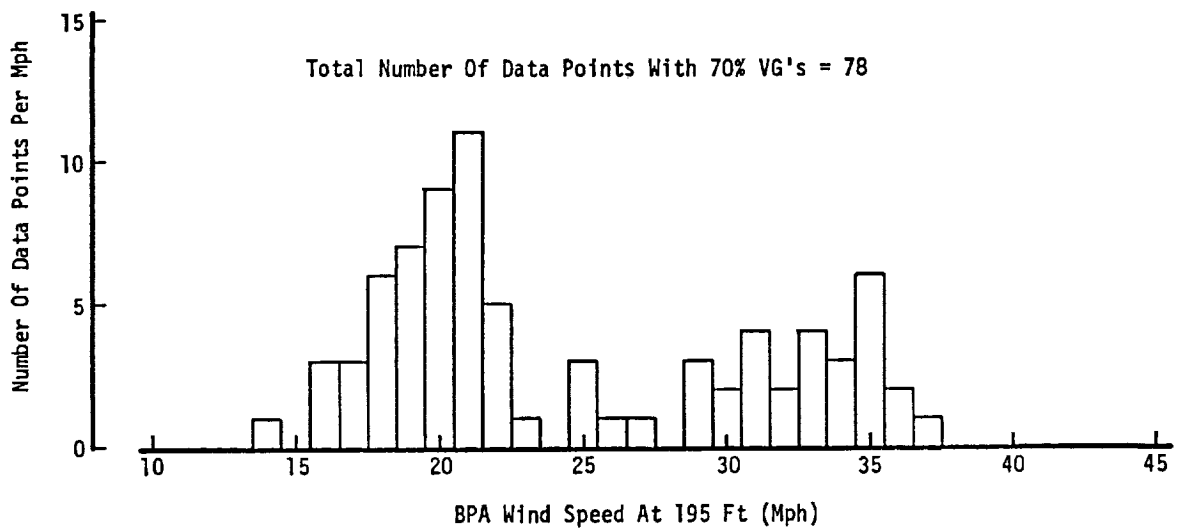


Figure 12. Data Point Distribution With 70% Vortex Generators.

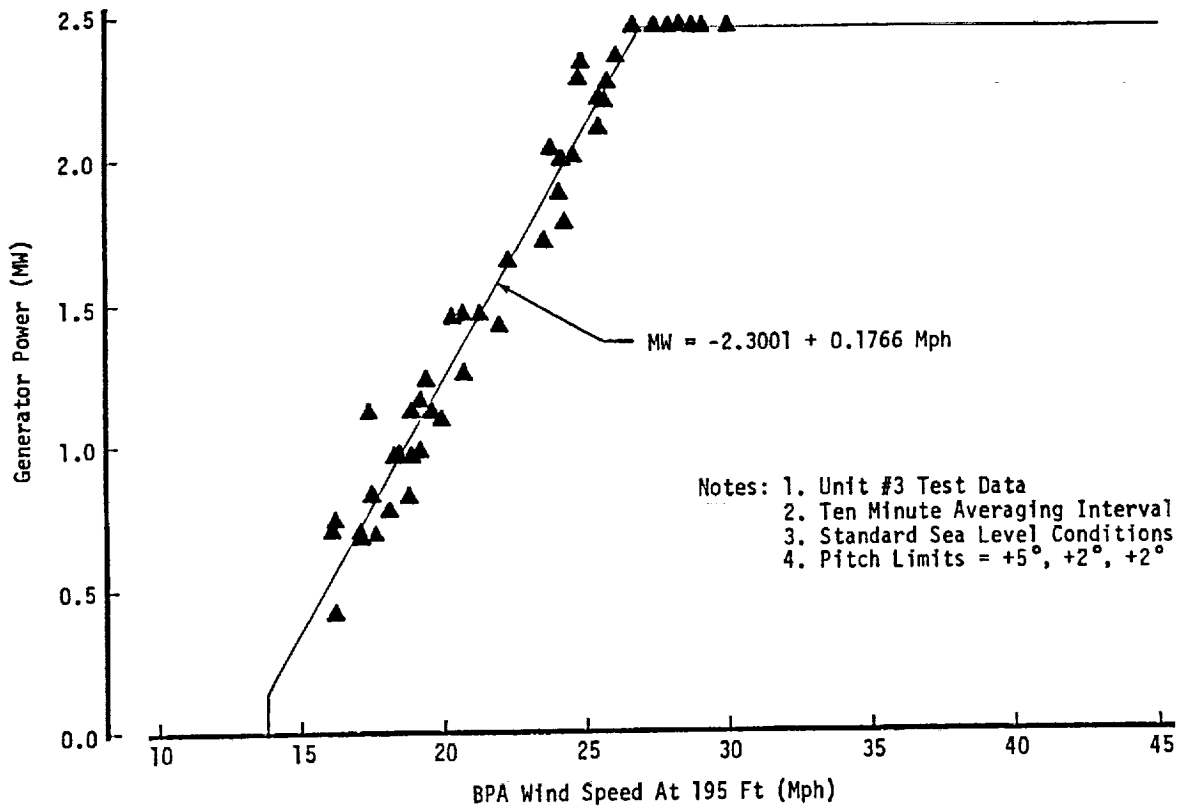


Figure 13. Mod-2 Power Performance With 100% Vortex Generators.

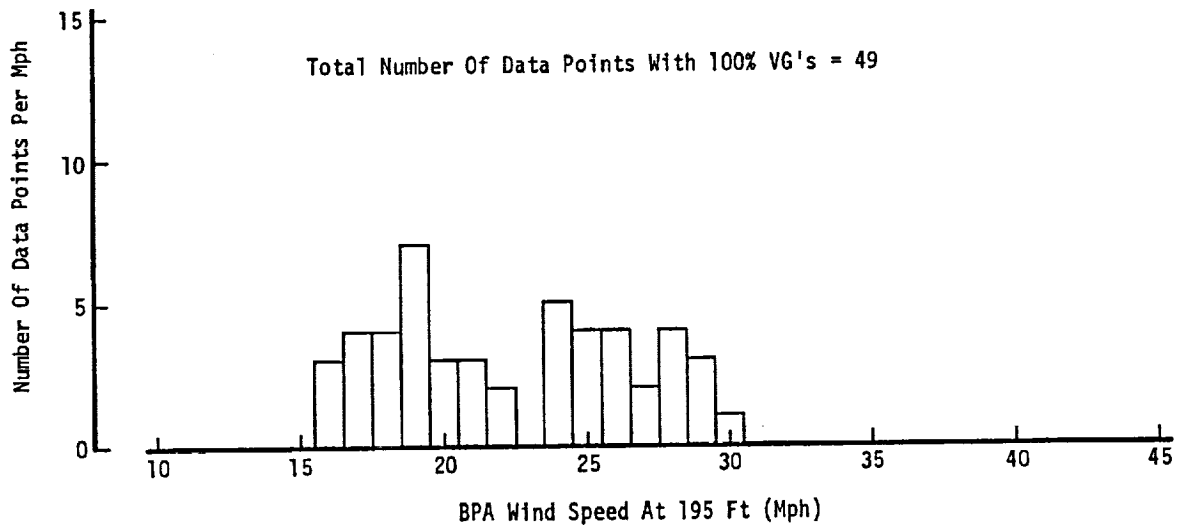


Figure 14. Data Point Distribution With 100% Vortex Generators.

Standard Sea Level Conditions

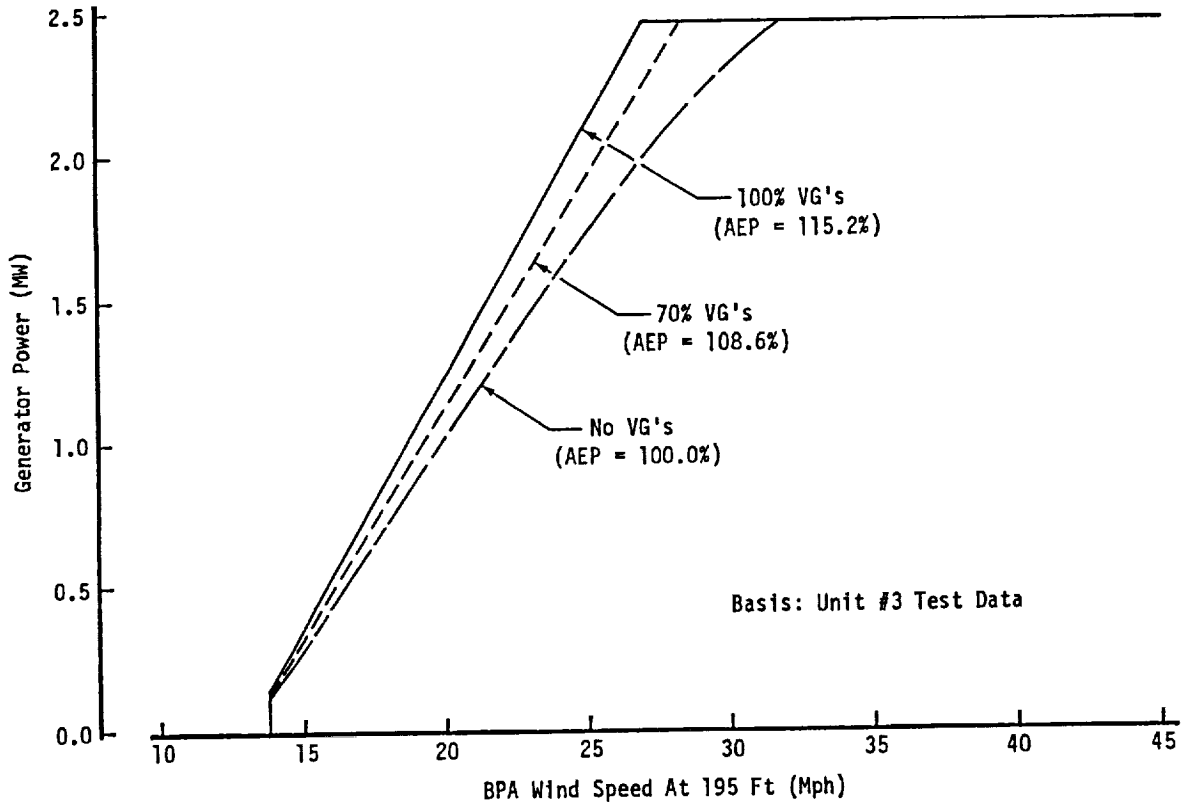


Figure 15. Mod-2 Power Performance Summary.

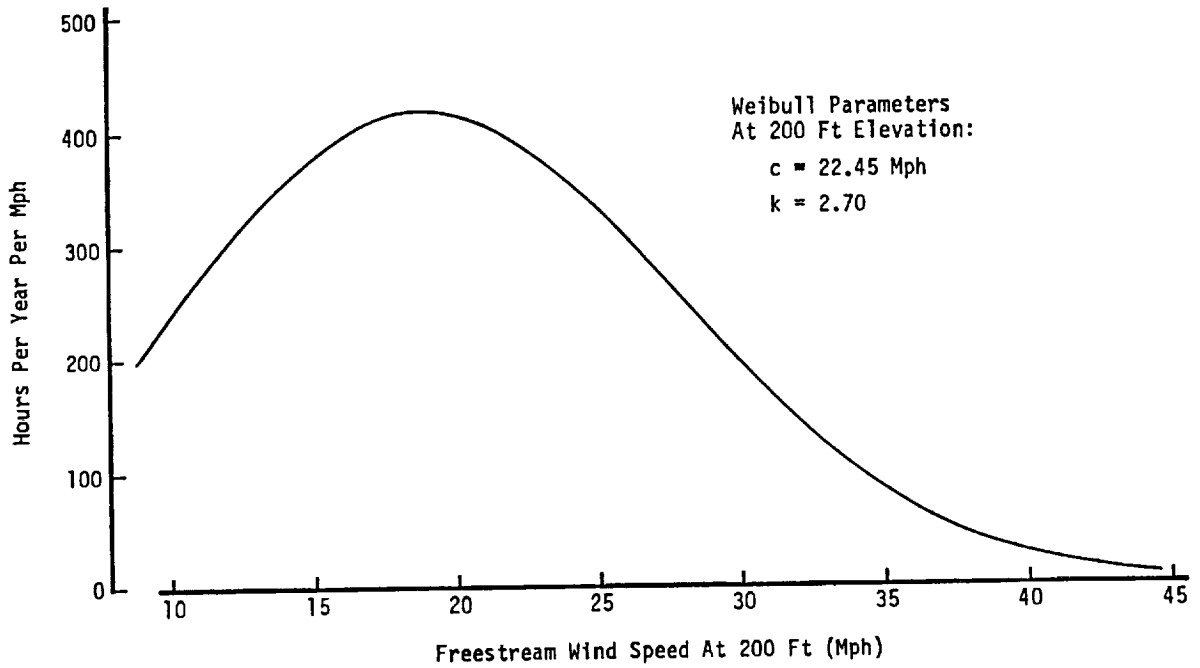


Figure 16. Mod-5B Weibull Wind Speed Distribution At 200 Ft Elevation.

